A Synoptic Study of Deformation Fields

By LAURI A. VUORELA, University of Stockholm[1]

(Manuscript received December 10, 1952)

Abstract

An attempt has been made to compute the field of horizontal deformation for a few synoptic situations. Some reasons for the rather high values of dilatation obtained are discussed and criticism over the method is presented.

When discussing the applicability of the vorticity theorem in numerical forecasting, the question arises concerning the magnitude of the deformation. If the vorticity is computed using a grid size of several hundreds of kilometers, it is necessary to make sure that the deformation is not so strong that important details in the flow pattern disappear between the grid points during the forecast interval. In order to illustrate this question the rate of horizontal deformation has been computed for a few synoptic situations.

The distribution of horizontal velocity around a given point in a plane surface at a given moment may be expressed by Taylor expansions of the x- and y-components (u, v) of velocity about the origin (see e. g. Handbook of Meteorology, p. 414). Neglecting derivatives of higher order we obtain after rearranging the terms

$$\begin{cases} u = u_0 - \dfrac{1}{2}\left(\dfrac{\partial v}{\partial x} - \dfrac{\partial u}{\partial y}\right) y + \dfrac{\partial u}{\partial x} x + \dfrac{1}{2}\left(\dfrac{\partial v}{\partial x} + \dfrac{\partial u}{\partial y}\right) y \\ v = v_0 + \dfrac{1}{2}\left(\dfrac{\partial v}{\partial x} - \dfrac{\partial u}{\partial y}\right) x + \dfrac{\partial v}{\partial y} y + \dfrac{1}{2}\left(\dfrac{\partial v}{\partial x} + \dfrac{\partial u}{\partial y}\right) x \end{cases} \tag{1}$$

Here the first terms on the right hand side represent the translatory field, the second terms the rotational field and the last two pairs of terms the deformation field. For the sake of brevity we may write.

$$\frac{1}{2}\left(\frac{\partial v}{\partial x} + \frac{\partial u}{\partial y}\right) = K \tag{2}$$

We shall here only consider the deformation and denote by u_1 and v_1 the corresponding velocity field, i. e.

$$\begin{cases} u_1 = \dfrac{\partial u}{\partial x} x + K y \\ v_1 = K x + \dfrac{\partial v}{\partial y} y \end{cases} \tag{3}$$

Let us choose a new coordinate system (1), the axes of which coincide with the axes of dilatation. Thus we may assume

$$\begin{cases} u' = \dfrac{\partial u'}{\partial x'} x + K' y' = \alpha x' \\ v' = K' x' + \dfrac{\partial v'}{\partial y'} y' = \alpha y' \end{cases} \tag{4}$$

For the sake of simplicity we omit the primes and may thus write

$$\begin{cases} \left(\dfrac{\partial u}{\partial x} - \alpha\right) x + K y = 0 \\ K x + \left(\dfrac{\partial v}{\partial y} - \alpha\right) y = 0 \end{cases} \tag{5}$$

[1] Written while on leave from the Institute of Meteorology, University of Helsinki.

From this system of equations α may be solved by putting the determinant equal to zero.

$$\alpha^2 - \left(\frac{\partial u}{\partial x} + \frac{\partial v}{\partial y}\right)\alpha + \frac{\partial u}{\partial x}\frac{\partial v}{\partial y} - K^2 = 0 \quad (6)$$

If we consider geostrophic motion, the divergence term $\frac{\partial u}{\partial x} + \frac{\partial v}{\partial y}$, or in this case $- v_g/a$ cotang φ (v_g denotes the geostrophic velocity, a is the radius of the earth, and φ is latitude) may be considered as a small quantity in comparison with the other terms.

Thus we obtain

$$\alpha = \pm \sqrt{K^2 + \left(\frac{\partial v}{\partial y}\right)^2} \quad (7)$$

Taking the positive sign of α it represents the intensity of dilatation per unit of time since $u' = \frac{dx'}{dt} = \alpha x'$ according to (4) and thus

$$x' = x'_0 e^{\alpha t} \quad (8)$$

Six hours has been chosen as unit of time and thus the deformation of the grid squares in six hours is obtained by multiplying the grid size l by e^{α}.

If ψ denotes the angle between the axis of dilatation and the x-axis, we obtain from (5), upper equation

$$(y/x)_{dil} = \operatorname{tg}\psi = \frac{\alpha + \partial v/\partial y}{K} \quad (9)$$

According to the geostrophic assumption

$$\begin{cases} u_g = -\dfrac{g}{f}\dfrac{\partial z}{\partial y} \\ v_g = +\dfrac{g}{f}\dfrac{\partial z}{\partial x} \end{cases} \quad (10)$$

where g denotes the acceleration of gravity, z the contour height of the isobaric surface and f the Coriolis parameter. Thus one has to compute

$$\frac{\partial v}{\partial y} = -\frac{\partial u}{\partial x} = \frac{g}{f}\cdot\frac{\partial^2 z}{\partial x \partial y} = m(\varphi)\,[A] \quad (11)$$

where $[A]$ is the numerical value of $g/f \cdot \partial^2 z/\partial x \partial y$ calculated from the values at the grid points (by means of finite differences) and $(m(\varphi))$ is a scale factor.

Similarly we obtain for K from (2)

$$K = \frac{1}{2}\frac{g}{f}\left(\frac{\partial^2 z}{\partial x^2} - \frac{\partial^2 z}{\partial y^2}\right) = 2\,m\,(\varphi)\,[B] \quad (12)$$

When the numerical values of K and $\frac{\partial v}{\partial y}$ are known we easily obtain α from (7) and further tg ψ from (9).

Any two-dimensional non-divergent velocity field may be decomposed in a translation, rotation and deformation. For some cases studied, the rotational field had been computed previously in connection with tendency computations using the barotropic vorticity equation. We may easily obtain the deformation by simply subtracting the translation and the rotational field from the geostrophic wind field given in our maps. This procedure was used as a check in one case.

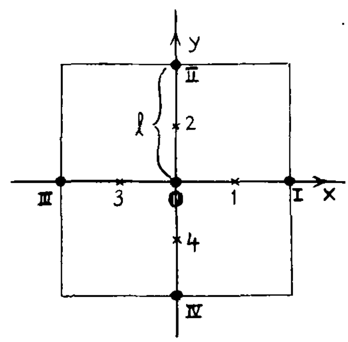

Fig. 1. A typical group of five neighbouring grid points used for evaluation of the derivatives.

The horizontal deformation has been computed for a set of grid points at four pairs of 500 mb maps. Two of these, Nov. 4, 1951, 0300Z—1500Z, and Dec. 5, 1951 1500Z— Dec. 6, 1951 0300Z represent situations, where the barotropic tendency computation was successful, the correlation coefficient between the computed and observed tendencies being 0.81 resp. 0.79. The two other pairs, Nov. 14, 1951 1500Z —Nov. 15, 1951 0300Z and Dec. 2, 1951 1500Z —Dec. 3, 1951 0300Z represent cases where the barotropic tendency computation failed with a correlation coefficient 0.06 resp. 0.13. In addition to these a few other maps have been used. For the sake of clarity the writer has, when drawing the figures, operated with small squares the size of them being about a half of the real size corresponding to the grid interval used, 314 km at latitude 50° N. All the drawings are not reproduced here, but the figures 2—3 represent a few typical cases showing the shape of the grid squares after six hours continuous and constant deformation.

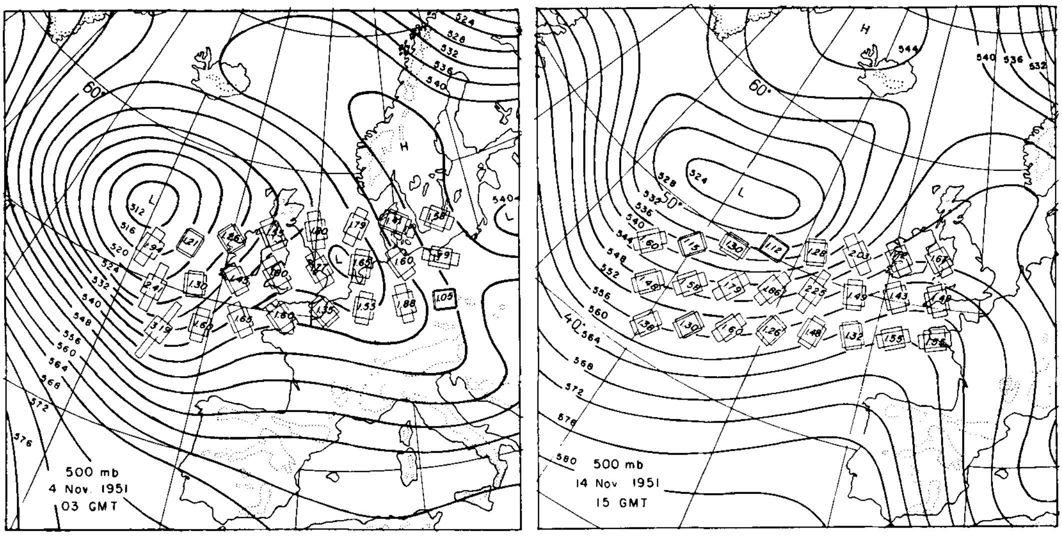

Fig. 2. Contours, labelled in tens of meters, interval 40 m, and figures, showing the horizontal deformation of the grid squares (in a reduced scale) a) 0400 GMT 4 November 1951; b) 1500 GMT 14 November 1951. The numbers inside of the squares represent the dilatation coefficients (see eq. (10) in the text).

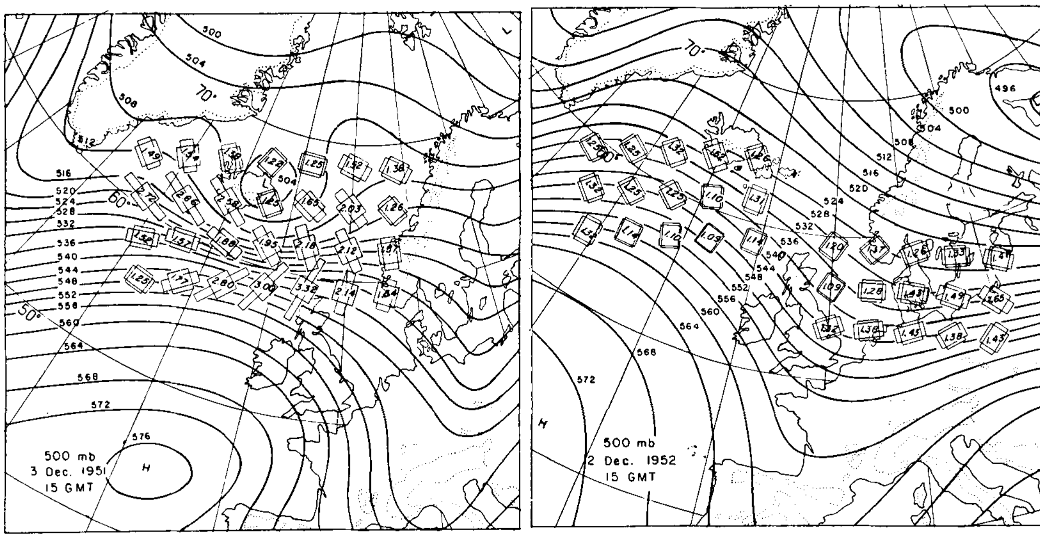

Fig. 3. Contours and deformation figures a) 1500 GMT 2 December 1951; b) 1500 GMT 3 December 1951. Notations as in Fig. 2.

When examining the distribution and shape of the deformation figures on the maps treated, it was hard to detect any systematic difference between the cases where the tendency computations were successful or where they failed. The maximum values obtained meant a horizontal dilatation of the order of three times in six hours, which is a rather high value. But on the average, the deformation seemed to be of the same order of magnitude in all cases investigated here and more or less unorganized. However, the number of the maps treated was not very great, which makes it difficult to draw any more general conclusions. The writer had also drawn the lines (not reproduced here) representing the distribution of the absolute vorticity at the beginning of the time interval used. Also the vorticity advection, and the corresponding isolines (not reproduced here) were calculated and plotted in order to see if the strongest deformation might coincide with the greatest vorticity advection. Yet, it was impossible to find any systematic correlation between these two quantities.

The question now arises about the real meaning of the deformation computed here. Since the motion was regarded as geostrophic and non-divergent, the deformation in the grid points does not exactly correspond to the deformation that would be obtained from actual wind data. It is easy to see that the geostrophic assumption sometimes must lead to severe errors. As an example we may select the case schematically shown in Fig. 4. In this figure

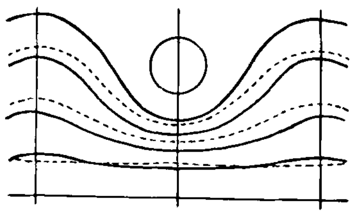

Fig. 4. A schematic picture showing the characteristic flow through a 400-mb trough.

the characteristic flow through a 500-mb trough from a western to an eastern ridge is represented by stream lines (dashed lines) and contours (full lines). The trough and ridge lines are stright lines and the stream-line and contour-line pattern are symmetric about the trough line. Nothing essential in the following qualitative discussion would change if a more general pattern would have been assumed. Furthermore we assume that the movement of the trough is small compared with the wind velocity.

The mutual pattern of stream lines and contours indicates that the air movement is accelerated from the western ridge to the trough and decelerated from the trough to the eastern ridge. This is a common distribution of velocity on the 500-mb chart. Thus there exists generally an ageostrophic component normally to the contours in all parts of the diagram except at the trough and ridge lines. This ageostrophic component is directed to lower contours between the western ridge and the trough and toward higher contours between the trough and the eastern ridge.

At the trough line the cross-stream acceleration is directed toward lower contours and at the ridge lines toward higher contours. Hence the ageostrophic component in the direction of the flow, or in the direction of the contour lines is positive on the ridge lines and negative on the trough line. This ageostrophic component has for steady state the value given by the upper formula of (13). The lower formula gives the approximate value of the normal component.

$$\left\{\begin{aligned} \triangle v_c &\approx \mp \frac{1}{f}\frac{v_c^2}{r} \\ \triangle v_n &\approx \frac{v_c}{f}\frac{\partial v_c}{\partial c} \end{aligned}\right. \tag{13}$$

Here v_c denotes the velocity in the direction of the contour lines, f is the Coriolis parameter and r the radius of curvature of the contour lines, positive for cyclonic curvature, negative for anticyclonic curvature. The absolute values of these components may vary between 0—10 m sec^{-1}. According to this the total ageostrophic flow is directed normally to the contours around the inflection points of the contour-line pattern, and parallel to the contours at the ridge and trough lines. At the ridge lines the ageostrophic wind is positive, at the trough line negative. Since the wind divergence is approximately equal to the divergence of the ageostrophic wind the assumption of non-divergence made previously cannot generally be true, if the ageostrophic components are considerable.

Since the ageostrophic component due to the curvature of the flow easily can reach values of 10—20% of the geostrophic component, or sometimes even higher values, the influence on the computed deformation can be considerable. A couple of examples of this will be given in the following. Since it is very difficult to compute exact values of the curvature of trajectories, the curvature of stream lines (or contour lines) has been used. This curvature may differ very much from the curvature of trajectories. Since our calculation here has been made in region with westerly wind components and since the disturbances are moving west-east the computations in most cases give too high values for the corrections. The computations have been made in following way. The geostrophic wind velocity has been measured using a conventional geostrophic wind scale at a sequence of points, with intervals of 100 km to west and east of a selected grid point, following the curvature of the contour lines. Then the radius of curvature has been measured as carefully as possible and a conventional scale is used for getting the corresponding gradient wind. The variation of the Coriolis parameter has been neglected. Both these velocity values are plotted against the distance between the points used. Figs. 5—6 are selected examples showing the velocity profiles computed around a few grid points taken from the maps presented in Figs. 2—3. The points are labeled from left to right beginning with the topmost row. The curves give directly the velocity difference per hour and per grid size and assuming a stationary state one can obtain the six hourly decrease in the distance between the western and eastern border of the grid square or with other words the magnitude of contraction, and compare it with the numerically computed values.

From Fig. 5 we can see, that at grid point number six (see the map in Fig. 2b), located at a place where the curvature of the contour lines is cyclonic (case a), the velocity difference is 28 km per hour and per unit distance when using the geostrophic velocity. This means, that assuming a stationary state, the grid size has in six hours been reduced with an amount

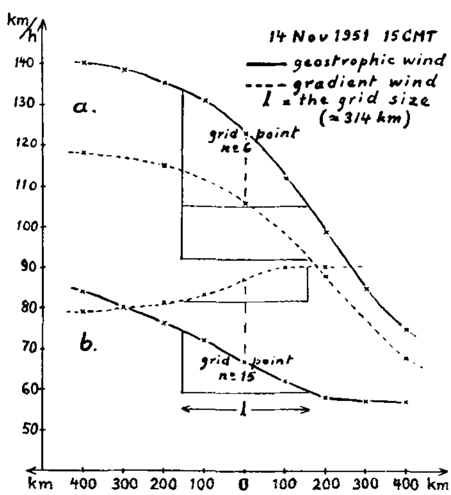

Fig. 5. Geostrophic and gradient wind profiles around two grid points on the 500-mb map at 1500 GMT 14 November 1951.

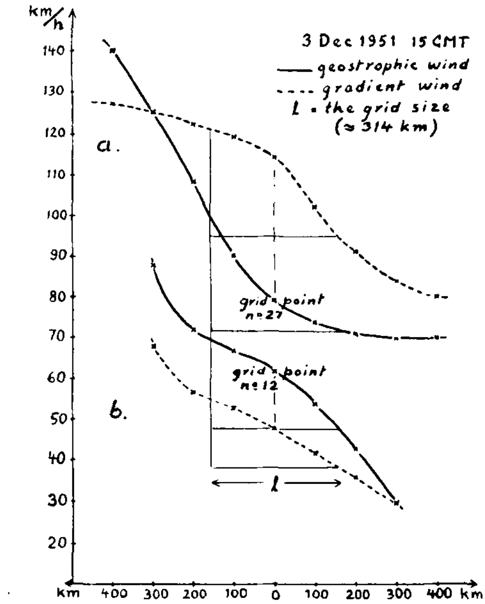

Fig. 6. Geostrophic and gradient wind profiles around two grid points on the 500-mb map at 1500 GMT 3 December 1951.

of 168 km, or to a length of 146 km. Using the numerically calculated coefficient of contraction, $e^{\alpha}=2.03$, we get the value of 155 km, which means a relative good agreement. But, making use of the gradient wind velocity, the corresponding figures are 22 km/hour and thus in six hours 132 km. This means that the grid size is reduced to a length of 182 km, which would correspond to a contraction coefficient that is considerably less, $e^{\alpha}=1.72$. It should be pointed out, however, that the divergence of the real wind may not be assumed to be equal to zero.

The contrast is still more striking, if we consider the grid point number fifteen (case b), where the curvature is changing from cyclonic to anticyclonic one. Here the geostrophic velocity difference, taken from the curve, gives a reduction of the grid size with 90 km in six hours or to a value of 224 km, which well agrees with the numerically calculated value of 220 km ($e^{\alpha}=1.43$). But in this case we have an increase of the gradient wind velocity in the direction of the flow. It leads to a dilatation in that direction with the grid size prolonged to a length of 362 km, which is quite in controversy with the results geostrophically computed.

The two other comparisons presented here are based on the map in Fig. 3 b. The velocity difference taken from the geostrophic wind profile around the grid point number twelve (case b in Fig. 6), where the curvature of the contour lines is cyclonic, would lead to a reduced l-value of 188 km. The corresponding numerical calculation ($e^{\alpha}=1.65$) gives 190 km. On the contrary, the gradient wind difference gives a value of 228 km, corresponding to a considerably less contraction coefficient $e^{\alpha}=1.38$. When the same procedure is applied at the point number 27 (case a in Fig. 6), where the curvature is anticyclonic, we obtain a graphically computed reduced l-value of 146 km versus the numerically calculated value of 147 km ($e^{\alpha}=2.14$). In this case the gradient wind difference gives 158 km, corresponding to $e^{\alpha}=1.99$.

From these examples one may conclude that the geostrophic assumption in many cases leads to too large deformations. Applying the previous results, e. g., on the area between a western trough and an eastern ridge the negative change of the geostrophic wind in the direction of the flow is generally greater than the change of the real wind. Consequently, both contraction and dilatation are exaggerated if we assume non-divergence. In the region between a western ridge and an eastern trough the opposite is true; here the dilatation in direction of the flow and the contraction normally to the direction are too great. HOVMÖLLER (1952) has in a recent paper stressed the importance of taking into account the cyclostrophic and other non-geostrophic wind components for the vorticity computations and recommends the more extensive use of observed winds. The same seems to hold also with regard to the deformation computations, although we are here merely dealing with the application of the geostrophic assumption in stead of the difficulties depending upon observational errors as treated by Hovmöller.

One might also expect an intensive concentration of isotherms and a corresponding remarkable frontogenesis over regions with strong computed deformation, but an examination of the maps showed that in general this was not the case. This further strengthens the impression that the values of deformation obtained with the method used are exaggerated. One has to keep in mind, however, that the neglect of vertical movements also is essential for the change of the isothermal pattern at a given level. It is a well known fact, that the isotherms do not commonly move with the speed of the wind. Considering, e. g., the isotherms on a series of upper air charts in the vicinity of the boundary between a warm and a cold air mass, we now from the practical experience that on the warm air side the movement of the isotherms is slower than the horizontal wind speed indicates, because of the ascending motion in the warm air. Correspondingly the isotherms on the cold air side move more slowly than the horizontal wind speed due to the subsiding motion there. Consequently, a dispersion of the isotherms may occur instead of a concentration. This is also easy to establish by the aid of the following consideration.

The individual rate of change of the temperature T with time t may be written

$$\frac{dT}{dt}=\frac{\partial T}{\partial t}+v_s\frac{\partial T}{\partial s}+w\frac{\partial T}{\partial z} \tag{14}$$

where v_s denotes the wind velocity in the direction of the flow, $\frac{\partial T}{\partial t}$ is the temperature change in the same direction, w is the vertical wind velocity and z the vertical coordinate.

If γ_d denotes the dry adiabatic lapse rate and γ the actual lapse rate, (14) may be written (see Panofsky, 1946)

$$\frac{\partial T}{\partial t}=-v_s\frac{\partial T}{\partial s}-w\,(\gamma_d-\gamma) \tag{15}$$

If we write

$$\frac{\partial T}{\partial t}=-c\frac{\partial T}{\partial s} \tag{16}$$

where c denotes the speed of the isotherms moving in the direction of the flow, we obtain

$$c\frac{\partial T}{\partial s}=v_s\frac{\partial T}{\partial s}+w\,(\gamma_d-\gamma) \tag{17}$$

and further

$$c=v_s+\frac{(\gamma_d-\gamma)}{\frac{\partial T}{\partial s}}\,w \tag{18}$$

Assuming $\dfrac{\gamma_d-\gamma}{\frac{\partial T}{\partial s}}$ to be a constant (which presumes equidistant isotherms) we can derive from (18)

$$\frac{\partial c}{\partial s} = \frac{\partial v_s}{\partial s} + \frac{(\gamma_d - \gamma)}{\frac{\partial T}{\partial s}} \frac{\partial w}{\partial s} \tag{19}$$

In (19) the first term on the right hand side, $\frac{\partial v_s}{\partial s} < 0$, because the flow in the warm air mass is stronger than in the cold air mass, $(\gamma_d - \gamma)$ is almost always > 0, $\frac{\partial T}{\partial s} < 0$ in the boundary between the warm and cold masses. Thus, $\frac{\gamma_d - \gamma}{\frac{\partial T}{\partial s}} < 0$. At last, $\frac{\partial w}{\partial s}$ is also negative, because we have an ascending motion on the warm air side, a descending motion on the cold air side. Hence, the second term on the right hand side of (19) is positive. Accordingly, the first and second terms on the right hand side have opposite signs. This means that the acceleration of the movement of the isotherms in the direction of the flow is less than the acceleration of the horizontal wind in agreement with the synoptic experience. However, this behaviour of the isotherms, primarily connected with the problem of the frontogenesis, will not be considered here in any more details.

Acknowledgements

The author wishes to express his thanks and appreciation to Professor C.-G. Rossby, the Chairman of the Institute of Meteorology, Stockholm University, at whose suggestion this study was initiated and to whom the author is indebted for his unfailing interest. Furthermore I wish to acknowledge the benefit received from many helpful and stimulating discussions of the problem with Dr A. Eliassen, Videnskaps-Akademiets Institutt for Vær- og Klimaforskning, Oslo, fil. lic. B. Bolin and fil. lic. G. Arnason, Institute of Meteorology, Stockholm University. The author is also greatly obliged to Professor E. Palmén, Academy of Finland, Helsinki, for many valuable suggestions and criticism.

REFERENCES

Hovmöller, Ernest, 1952: A Comparison between Observed and Computed Winds with Respect to their Applicability for Vorticity Computations. *Tellus*, **4**, 126—134.

Panofsky, H. A., 1946: Methods of Computing Vertical Motion in the Atmosphere. *J. Meteor*, **3**, 45—49.